ISSN 1027-5495. Functional Materials, 30, No.3 (2023), p. 350-355.
doi:https://doi.org/10.15407/fm30.03.350

Study of the effect of doping with (Zn,Tc) on the electronic and optical properties of $FeNi_3$ alloys: ab-inition calculation

***Yamina Benkrima*[1], *Abdulhadi Mirdan Ghaleb*[2], *Djamel Belfennache*[3], *Radhia Yekhlef*[3], *Afif Benameur*[4]**

[1]Ecole Nrmale Superieure de Ouargla, 30000 Ouargla, Algeria
[2]Department of Physics, College of Science, University of Kirkuk, Iraq
[3]Research Center in Industrial Technologies CRTI, P.O. Box 64, Cheraga, 16014 Algiers, Algeria
[4]Faculty of Science and Technology, University of Mustapha Stambouli of Mascara, 29000, Algeria

Received April, 13, 2023

The structural, electronic and optical properties of the $FeNi_2Zn$ and $FeNi_2Tc$ alloys were studied using the first-principles planar wave method compatible with the ultrasoft pseudopotential scheme under the density functional theory (DFT). The calculated equilibrium lattice constant for $FeNi_3$ is very close with other available results. It turns out that the large contribution of *d* electrons to the total electronic density of states is dominant, which in turn affects the electronic and magnetic properties of these alloys. The electronic band structure, total and partial electron density were analyzed and it was concluded that the $FeNi_2Tc$ alloy has greater magnetic properties; absorption coefficient, optical conductivity, and refractive index were calculated for both alloys.

Keywords: density functional theory DFT, $FeNi_2Zn$, $FeNi_2Tc$, electronic properties, magnetic properties, optic properties.

Дослідження впливу допування (Zn,Tc) на електронні та оптичні властивості сплава $FeNi_3$: розрахунок ab-inition. *Yamina Benkrima, Abdulhadi Mirdan Ghaleb, Djamel Belfennache, Radhia Yekhlef, Afif Benameur*

Структурні, електронні та оптичні властивості сплавів $FeNi_2Zn$ і $FeNi_2Tc$ досліджені з використанням первинного методу плоских хвиль, сумісного зі схемою ультрам'якого псевдопотенціалу в рамках теорії функціональної щільності (DFT). Визначена рівноважна постійна решітки для $FeNi_3$ дуже близька до інших доступних результатів. Показано, що великий вклад *d*-електронів у загальну щільність електронних станів є домінуючим, що, у свою чергу, впливає на електронні та магнітні властивості цих сплавів. Проаналізовано електронну зонну структуру, повну та часткову електронну щільність, і зроблено висновок, що сплав $FeNi_2Tc$ має високі магнітні властивості, розраховано та проаналізовано коефіцієнт поглинання, оптичну провідність та показник переломлення двох сплавів.

1. Introduction

Over the past decade, metallic alloys have been the focus of many studies due to their potential applications in many fields: magneto-optical recording technologies [1, 2], magnetic media [3], magnetic sensors [4], and catalytic applications [5]. The most attractive forms of these alloys are nanoparticles and thin films [6]. The main factor that attracts attention to them is the variety of magnetic properties and the abil-

ity to control their parameters by adjusting the formula and conditions for their growth. For example, if these alloys have the following properties: large saturation magnetization (M_s), high Curie temperature (T_C), and large magnetic anisotropy energy (MAE), then they can be used in many technological applications such as electric motors and electronic devices storage [7].

Shuttleworth [8] employed the spin-polarized density functional theory (DFT) to study the band structure of binary Pt_xM_{1-x} (M = Fe, Co, and Ni) alloys in the ordered L12 and L10 phases. Burzo et al. [9] studied the band structure and magnetic properties of FePd ordered compounds using first-principles calculations. Their calculations for magnetic moments are in very good agreement with the reported experimental values. The lattice dynamic, thermodynamic and magnetic properties of some of them have been studied for different important phases of the Fe–Ni alloy such as L12 $FeNi_3$, taenite L10 FeNi and L12 Fe_3Ni using the density functional theory method [10]. Recently, the structural constants, elastic, electronic and magnetic properties of three Fe–Ni binary metals ($FeNi_3$, FeNi and Fe_3Ni) under pressure change were studied by M.J.Wang et al. [11] using the first principle DFT.

In this work, structural, electronic, magnetic and optic properties of $FeNi_2Zn$ and $FeNi_2Tc$ alloys are investigated using exchange-correlation approximations of GGA. This work includes calculating lattice parameters, bulk modulus, the total and partial density of states, bands structures, total magnetic moment, absorption coefficient and optical conductivity. The achieved results are discussed and compared to the available experimental and theoretical values.

2. Experimental

In this work, the calculations are based on the principles of the density functional theory (DFT) of spin-polarized states [12, 13]. In terms of exchange and correlation functional, the Generalized Gradient Approximation (GGA) functional was applied in accordance with the proposals of Perdew, Burke and Ernzerhof (PBE) [14]. An increase in geometries of alloys was made through the functional density first principle-simulations technique, which is rooted in the numerical atomic orbital method according to SIESTA code implementation [15, 16]. The structures of the alloys were drawn using the XCRYSDEN program code. The extended wave functions were used in the plane wave fundamental ensembles using kinetic energy cutoffs of 400 eV. This was applied to all systems included in our research. The Monkhorst-Pack grid having special k-point meshes was used to carry out the integrations of the Brillouin zone. As for the implementation of self-consistent field calculations, a criterion of convergence estimated at 10^{-4} to total energy was chosen for this purpose. Actually, 0.02 Å was the value of the maximum tolerance for ion displacement in the alloys. We obtained the optimized structures of all alloys when the atomic forces were less than 0.004 eV/Å. Z-matrices in the Q-Chem program output provided the optimized electronic structure for each alloy. However, we calculated the electronic properties based on both the total electronic energy and the self-consistent field (SCF) orbital energy values. We used the total energies of the optimized alloys to find out the formation energy, band structure energy, total density of states and partial density of states, as well as some optical properties of these alloys.

3. Results and discussion

3.1. Optimized structures

Structural parameters of an originally relaxed @$FeNi_3$ cell with a space group of Pm3m, in cores with four atoms are defined by the following reduced coordinates: Fe (0, 0, 0) and three numbered for rested Ni atoms Ni_1 (1/2, 1/2, 0), Ni_2 (0, 1/2, 1/2), Ni_3 (1/2, 0, 1/2). The lattice constants of $FeNi_3$ alloy over the past decades have been verified many times; the basic structure of the stable $FeNi_3$ alloy is the $Pm3\overline{m}$ group structure and the lattice constants are $a = b = c = 3.548$ Å, $\alpha = \beta = \gamma = 90.00°$. Whereas in our present work, we find the lattice parameters for the new alloy $FeNi_2Zn$ as $a = b = c = 3.534$ Å, while alloy $FeNi_2Tc$ has $a = b = c = 3.569$ Å.

In our calculations, we used the Siesta code to find the initial cell constants for $FeNi_3$, $FeNi_2Zn$ and $FeNi_2Tc$ alloys, where we replaced one of the nickel atoms with zinc (Zn) atom for the first time and a technetium (Tc) atom for the second time to obtain $FeNi_2Zn$ and $FeNi_2Tc$ alloys. In this section, the results obtained were compared with experimental results as well as previous theoretical works, and we present the structural parameters of the primary $FeNi_3$ cell in Table 1 Also we obtained the lattice parameters of a $FeNi_3$, $FeNi_2Zn$ and $FeNi_2Tc$ (see Fig. 1).

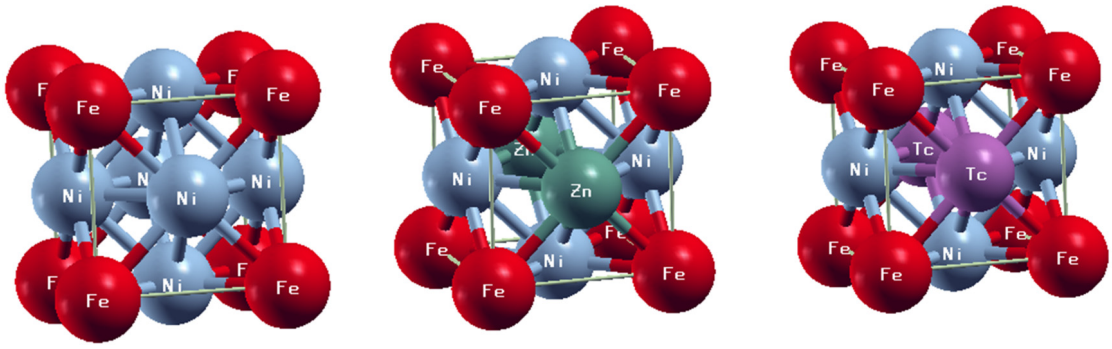

Fig. 1. Structures: (a) $FeNi_3$, (b) $FeNi_2Zn$, (c) $FeNi_2Tc$.

Table 1. Structural parameters of the optimized $FeNi_3$, $FeNi_2Zn$ and $FeNi_2Tc$ alloys compared with heoretical and experimental results

	work	*a*, Å	*b*, Å	*c*, Å
$FeNi_3$	Our work	3.528	3.528	3.528
	Theor [12]	3.548	3.548	3.548
	Exp [13]	3.55	3.55	3.55
$FeNi_2Zn$	Our work	3.534	3.534	3.534
$FeNi_2Tc$	Our work	3.569	3.569	3.569

What has been concluded from Table 1 is that the results reached are close to previous theoretical and experimental works and that doping $FeNi_3$ alloy with atoms of zinc (Zn) or technetium (Tc) changes the dimensions of the original cell and thus will increase its volume.

3.2. Electronic properties

3.2.1 Structure of energy

In order to study the basic structure, we choose a region called the Brillouin zone in order to find the electronic properties of the material. The Brillouin zone is a cube. It is noteworthy that further, the study of properties in this region can be extended to $FeNi_2Mn$ and $FeNi_2Cr$.

In our work we used the density function theory DFT and generalized gradient approximation GGA in order to determine the band gap value of $FeNi_2Zn$ and $FeNi_2Tc$, and we used this method because it is one of the most appropriate ways to study the electronic structures of materials. The structure of the energy bands of the alloys is shown in Fig. 2.

What can be seen in Fig. 2a and 2b, where the highest valence bands overlap with the conduction bands, and this is evidence of the metallic property of the two alloys. We find that both alloys have ferromagnetic properties, with magnetic moments estimated to be values of 5.49 μB and 5.63 μB for $FeNi_2Zn$ and $FeNi_2Tc$, respectively.

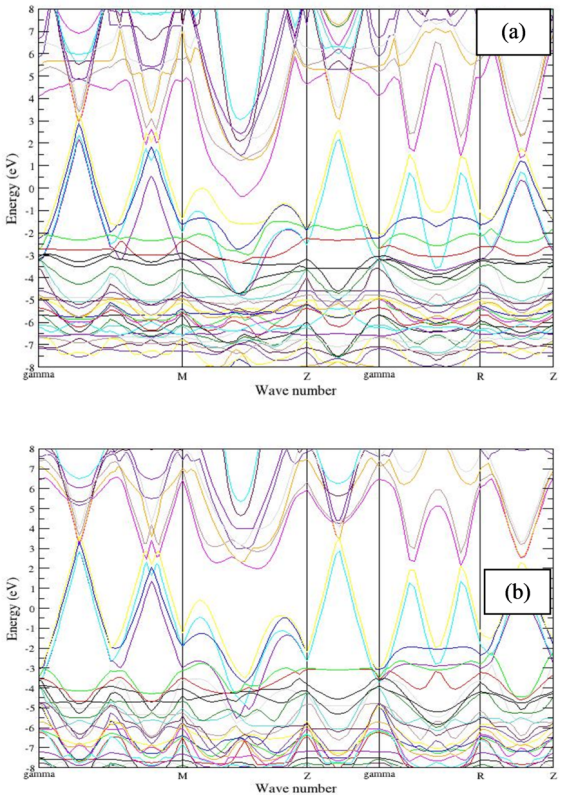

Fig. 2. Structure of energy bands: (a) $FeNi_2Zn$, (b) $FeNi_2Tc$.

3.2.2. Electronic density of states (DOS)

We plotted both the total density of states (TDOS) and the partial density of states (PDOS) for both $FeNi_2Zn$ and $FeNi_2Tc$ alloys using the GGA approximation and then analyzed them to determine the cause of the states that formed valence and conductive bands to understand the nature of the interactions between the atoms of the studied alloy, as shown in Fig. 4 and Fig. 5, respectively.

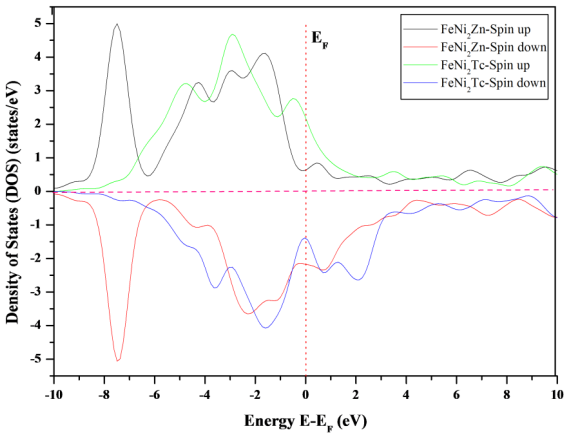

Fig. 3. Total density of states (TDOS): (a) $FeNi_2Zn$, (b) $FeNi_2Tc$.

Figure 3 shows that the calculated TDOS for $FeNi_2Zn$ and $FeNi_2Tc$ has high values with the GGA approximation in the region close to the Fermi level. It is clear from the figure that the TDOS value of $FeNi_2Tc$ is higher than that of $FeNi_2Zn$ in the region close to the Fermi level; this indicates that its valence band is rich in electrons. Close to the Fermi level, we recorded the highest peak density of states in the $FeNi_2Tc$ alloy, which was estimated to be 4.69 (state/eV), while the value 4.13 (state/eV) was recorded as the highest value for the $FeNi_2Zn$ alloy. It is at the Fermi level that the highest value of the density of states was also recorded in the $FeNi_2Tc$ alloy, the value of which is estimated at 2.36 (states/eV).

3.2.3. Partial density of states (PDOS)

In this work, we have calculated and analyzed the partial density of states (PDOS) of $FeNi_2Zn$ and $FeNi_2Tc$ alloys in order to understand the movement of electrons close to the Fermi level. Figures 4a and 4b show the PDOS of $FeNi_2Zn$ and $FeNi_2Tc$ respectively.

In the figure above, we present the density of states per atomic valence orbital (PDOS) in order to compare them with each other. Based on the different distributions of spin states (spin up and spin down) represented in the figure, the spin polarization is determined starting with a single primitive cell and later generalizing to each of the atomic domains; also, the role of electrons in different atomic valence orbital is revealed and their effect on the electronic properties. In order to better understand how the contributions of Fe, Ni, Zn and Tc atoms make up the $FeNi_2Zn$ and $FeNi_2Tc$ alloys, we calculated the expected density of states across electron orbitals as a function of energy ($E - E_F$).

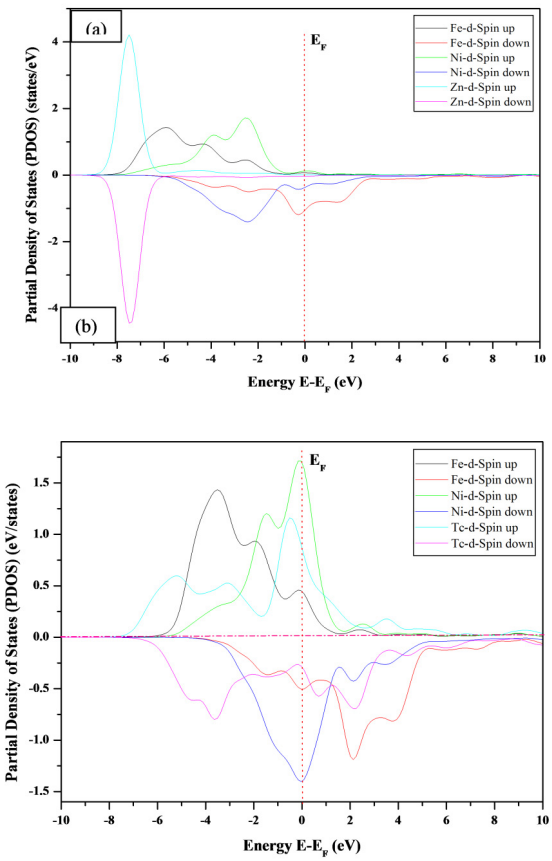

Fig. 4. Partial density of states (PDOS) for: (a) $FeNi_2Zn$, (b) $FeNi_2Tc$.

From the PDOS distributions, shown in Figs. 4a and 4b, for the $FeNi_2Zn$ alloy, it can be shown that the electronic states are mainly located in the region of high activity, extending from −9 eV to +2.5 eV around the Fermi levels. To give more detail, near the Fermi level, Ni atoms have larger 3-*d*-orbital states than Fe atoms; also, the contributions of the Ni spin-up 3-*d* electrons are larger than those from the same spin-down 3-*d* elements. The terminal contribution of 3-*d*-orbitals from all atoms is also dominant in the electronic distribution of $FeNi_2Zn$ and $FeNi_2Tc$ alloys. Also, the two atoms (Zn and Tc) have a high electronic distribution near the Fermi level, and the effect of the Tc atom in the electronic distribution in the alloy $FeNi_2Tc$ is greater.

It is very clear from the two Fig. 4a and 4b that zinc (Zn) or technetium (Tc) atoms added to the original $FeNi_3$ alloy has added a lot into the electronic distribution in the region close to the Fermi level, and the alloy $FeNi_2Tc$ is considered the best in terms of chemical and catalytic activity compared to the alloy $FeNi_2Zn$.

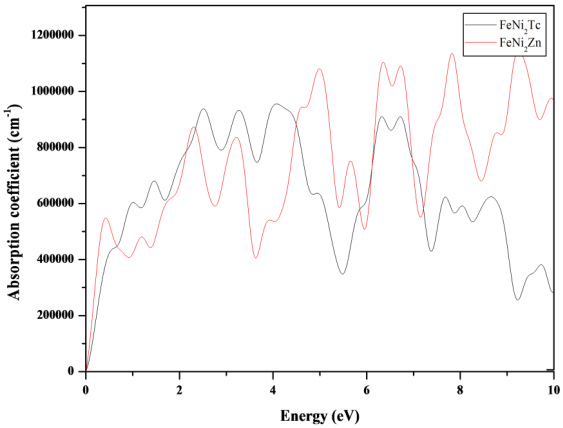

Fig. 5. Absorption coefficient of $FeNi_2Zn$ and $FeNi_2Tc$.

3.3.Optical properties

The study of the optical properties is very important; its importance lies in obtaining information about the values of the optical constants of the material and its relationship to the photons falling on it. We can use this information to design and manufacture optical blocks and optical pulses using different technologies.

3.3.1. Absorption coefficient

The absorption coefficient expresses the decrease in the energy spectrum of the incident radiation per unit distance in the direction of wave propagation in the medium. It is related to the energy of the incident photons. Through it, the nature of electronic transitions can be known, and its equation is of the form:

$$\alpha = \frac{4\pi K}{\lambda}, \qquad (1)$$

where α is the absorption coefficient, K is the coefficient of extinction and λ is wave length (cm). The adsorption coefficient values for $FeNi_2Mn$ and $FeNi_2Cr$ alloys were calculated with approximations of GGA, and they are shown in Fig. 5.

Figure 5 shows the change in the absorption coefficient as a function of the energy of the incident photon on the $FeNi_2Zn$ and $FeNi_2Tc$ alloys. It is clear from the figure that the absorption coefficient in general begins to increase gradually and in an oscillating manner with an increase in the energy of the photons of light, until the energy value 0.33 eV for the $FeNi_2Zn$ alloy and the value 1.05 eV for the $FeNi_2Tc$ alloy; after that the value of the absorption coefficient decreases significantly with an increase in the energy of the incident photons. After that, the values of the absorption coefficient fluctuate, decreasing and increasing in magnitude in terms of the energy of the incident photon. In general, the behavior of both alloys in absorption is almost the same, except that higher values are recorded sometimes in $FeNi_2Zn$ alloy; this is especially when the energy is 9.38 eV with a peak value at 1152000 cm^{-1}. This indicates that the change in the energy of the incident photons leads to different optical behavior in this material. This result is close to work [17].

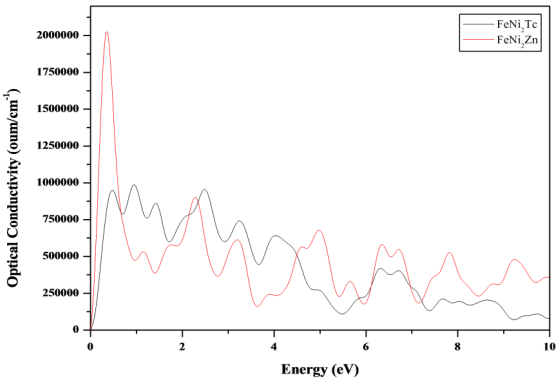

Fig. 6. Optical conductivity of $FeNi_2Zn$ and $FeNi_2Tc$.

3.3.2. Optical conductivity

It is a physical property that relates the current density to the electric field, and is given by the following equation:

$$\sigma(\omega) = \frac{J(\omega)}{\varepsilon(\omega)}, \qquad (2)$$

where σ is the optical conductivity (Sm/m), J is the current density (A/m^2) and E is electric field (N/C).

The optical conductivity values of $FeNi_2Zn$ and $FeNi_2Tc$ alloys have been calculated with approximations of GGA, and the results are shown in Fig. 6.

Figure 6 represents the optical conductivity changes in terms of the energy of photons falling on the $FeNi_2Zn$ and $FeNi_2Tc$ alloys using the GGA approximations. In general, we notice that the value of photoconductivity increases with increasing energy of the two alloys until energy 0.26 eV and 0.33 eV for $FeNi_2Zn$ and $FeNi_2Tc$ alloys respectively. In general, we find the optical conductivity curves of the two alloys almost identical, and the values fluctuate between increasing at times and decreasing at other times. If we compare the two alloys with each other, we find that the $FeNi_2Zn$ alloy is more optically conductive in the infrared

and visible ranges. It can generally be concluded from the analysis of both the absorption and optical conductivity curves, that the $FeNi_2Zn$ alloy has a good absorption value that allows its use in optoelectronics and photovoltaic composites.

4. Conclusions

• Based on density function theory (DFT) calculations and using the generalized gradient approximation (GGA) and the Siesta program, the results obtained for $FeNi_2Zn$ and $FeNi_2Tc$ alloys were compared in terms of structure, electrical and optical properties, and it was concluded that:

• The structural parameters of the alloys $FeNi_2Zn$ and $FeNi_2Tc$ differ from the structural parameters of the original alloy ($FeNi_3$). The results of the latter are in agreement with the results of previous studies.

• From the results of the total states density, it was found that the two alloys have metallic properties, in addition to the $FeNi_2Tc$ alloy which has a larger magnetic moment.

• Through the results of the partial density of states obtained for the two alloys, we found that the contribution of the 3-*d* orbital is dominant which in turn will affect the electronic and magnetic properties of the two alloys.

• Due to the differentiation in the optical properties of the two alloys, we find each has specific technological uses.

References

1. M.Futamoto et al., *AIP Adv.*, **6**, 85302 (2016).
2. K.M.Krishnan et al., *J.Appl.Phys.*, **83**, 6810 (1998).
3. K.M.Krishnan et al., *J.Mater.Sci.*, **41**, 793 (2006).
4. I.Koh, *Sensors*, **9**, 8130 (2009).
5. M.Neamtu et al., *Sci.Rep.*, **8**, 6278 (2018).
6. R.Ferrando, J.Jellinek, R.L., *Chem.Rev.*, **108**, 845 (2008).
7. A.Edstrom et al., *Phys.Rev.B*, **90**, 14402 (2014).
8. I.Shuttleworth, *Magnetochemistry*, **6**, 61 (2020).
9. E.Burzo, P.Vlaic, *J.Optoelectron.Adv.Mater.*, **12**, 1869 (2010).
10. N.Y.Pandya, A.D.Mevada, P.N.Gajjar, *Comput.Mater.Sci.*, **123**, 287 (2016).
11. M.J.Wang, G.W.Zhang, H.Xu, *J.Phys.Conf.Ser.*, **1507**, 082026 (2020).
12. D.Ruibin, C.Xiaoshuang, Z.Huxian et al., *J.Phys.B:At.Mol.Opt.Phys.*, **44**, 035102 (2011).
13. U.G.Gabriel, A.C.Reber, S.N.Khanna, *New.J.Chem.*, **37**, 3928 (2013).
14. Y.Benkrima, A.Ouahab, *Der Pharma Chemica.*, **9**, 62 (2017).
15. J.M.Soler, R.B.Marcela, M.Karo et al., *Phys.Rev.B*, **61**, 5771 (2000).
16. J.M.Soler, E.Artacho, J.D.Gale et al., *J.Phys.Condens.Matter.*, **14**, 2745 (2002).
17. B.Nourozia, A.Aminian, N.Fili et al., *Results in Physics*, **12**, 2038 (2019).